UNIVERSITY POLITEHNICA OF BUCHAREST

Doctoral School of Electronics, Telecommunications and Information Technology

Decision no. from

PhD DISSERTATION EXTENDED ABSTRACT

Ing. Andreea CONSTANTIN (PLĂTICĂ)

SEPARAREA EFECTULUI CURENȚILOR DE MOD COMUN DE PE CABLURILE DE ALIMENTARE ALE ANTENELOR DIN CÂMPUL TOTAL RADIAT

DISCRIMINATION OF COMMON MODE CURRENTS EFFECT ON ANTENNA FEEDERS FROM THE TOTAL RADIATED FIELD

DISSERTATION COMMITTEE

Prof. Dr. Ing. Bogdan IONESCU Univ. Politehnica from Bucharest	President
Prof. Dr. Ing. Răzvan TAMAȘ Univ. Politehnica from Bucharest	Advisor
Prof. Dr. Ing. Tudor PALADE Univ. Tehnică from Cluj-Napoca	Reviewer
Conf. Dr. Ing. Nicolae LUCANU Univ. Tehnică "Gheorghe Asachi" from Iași	Reviewer
Conf. Dr. Ing. Alina BĂDESCU Univ. Politehnica from Bucharest	Reviewer

BUCHAREST 2021

Contents

Chapter 1

Introduction

The separation of the effects produced by electromagnetic radiation from several sources has many practical applications. These may include the following:

a) radio-astronomy;
b) radio-location;
c) electromagnetic compatibility;
d) antenna measurement; the characterization of the antennas involves not only the evaluation of the field generated by the self-radiant elements, but also the study of the influence that their feeding circuits have on the global radiation pattern.

1.1 Presentation of the PhD domain

The design of an antenna involves the following steps:

1) defining a theoretical concept based on which the shape of the radiant elements is established; this stage it is either a process of synthesis or optimization of an existing architecture that allows to obtain certain values of the parameters that characterize the radiation.

2) simulation of the designed structure; in general, at this stage the antenna is characterized using a specialized software and does not take into account a possible contribution to radiation of the interconnection elements (connectors, feeding lines).

3) experimental validation, through measurements, of the designed antenna; in this stage the antenna is characterized by measurements either in a controlled environment (anecoid chamber) or *in situ*. Sometimes, however, the antenna-range measurements cannot reproduce the conditions of the final application, which leads to altered results by measuring not only the radiation of the antenna itself, but also the common currents that may occur on the feeding lines.

In this situation it becomes necessary to separate the effects of the radiated fields generated by the two sources and to identify methods to eliminate the radiation effects of the interconnecting elements, respectively.

1.2 Purpose of the PhD work

The purpose this work is to develop some methods that allow to discriminate the radiation generated by the common mode currents (occur on the outer conductor of the feeder) from the antenna radiation.

Methods to measure the field generated by common currents and to reduce their effect in antenna measurement systems will be investigated.

Regarding the effect discrimination, two directions will be addressed: one that exploits a possible orthogonality of the polarization of the two sources, and another that allows the separation of the two effects due to the variability of the common mode currents depending on the distance.

The case studies will cover both the situation in which the common mode currents occur when feeding a symmetric antenna through an asymmetric line, or when feeding a a monopole antenna on a small ground plane. In turn, the types of symmetrical antennas analyzed will have a different number of symmetry degrees.

1.3 Dissertation content

C hapter 1 presents the general introduction of the thesis, the PhD domain and the purpose of the thesis.

Chapter 2 presents an overview on the methods for evaluating the field generated by common mode currents. Both methods for measuring the radiation field, and methods for reducing the effect of common mode currents, existing in the literature, are presented.

In chapter 3, two types of antennas are theoretically investigated. This antennas (biconical and loop antenna) are the optimal solutions for the measurement methods proposed in the following chapters.

The fourth chapter describes a method for polarization separation of the radiated field produced by the antenna from that produced by the common mode currents on the outer conductor of the feed cable, in an multiple propagation paths environment. The proposed mmethod in validated by comparing the results with those provided by the time-gating method.

Another method that can be successfully applied to discriminate the common mode currents effect on antenna feeders from the total radiated field, is presented in chapter 5. Several strategies for the application of the method are developed, both for symmetrical antennas with different symmetry degrees and for monopole antennas on small ground plane.

Finally, in the chapter 6 the work is concluded, the results and the original contributions are highlighted and perspectives are drawn towards the future progress that could be done.

Chapter 2

Evaluation of common mode currents radiated field

2.1 Electromagnetic field generated by common mode currents

When feeding symmetrical antennas or electrically small antennas through asymmetrical transmission lines (e.g., coaxial cables), common mode currents may occur on the outer conductor of the feeder [1]. Common mode currents should normally be kept at least ten times smaller than the feed currents, in order to avoid undesirable effects. However, it has been shown [2] that common mode currents may have magnitudes comparable to the feed currents when the antenna size is comparable to the ground size or to the feed line length, and therefore have a major impact on the total radiated field.

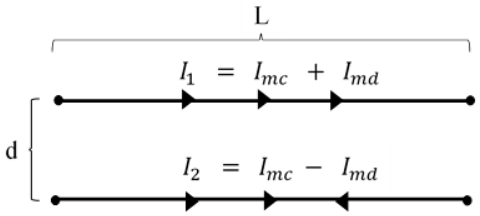

Figure 2.1 *Common mode currents and differential mode currents*

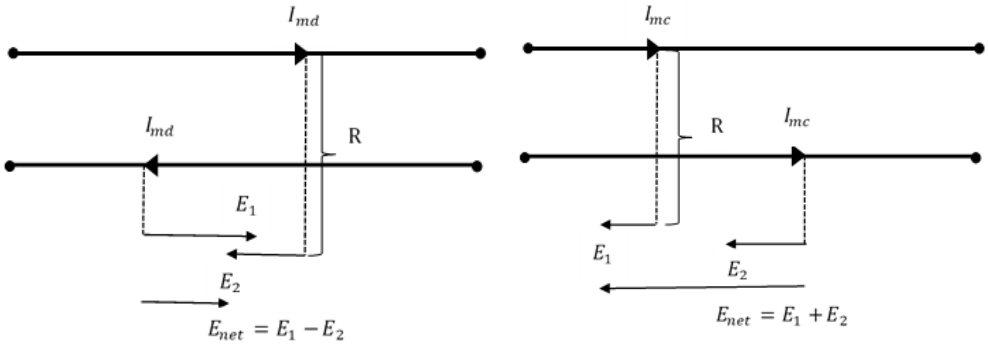

Figure 2.2 *Electric field generated by common and differential mode currents*

If the wires are electrically short, $L \ll \lambda$, then we may approximate each structure as two current elements.

$$\left|E_{D_{max}}\right| = \frac{120\pi^2}{{c_0}^2}\frac{I_{md}Ldf^2}{R} = 1.316\times10^{-14}\frac{I_{md}Ldf^2}{R} \quad \text{V / m.} \tag{2.22}$$

$$\left|E_{C_{max}}\right| = \frac{120\pi I_{mc}Lf}{{c_0}^2 R} = 1.257\times10^{-6}\frac{I_{mc}Lf}{R} \quad \text{V / m.} \tag{2.24}$$

Accurate predictions of the radiated emissions from common-mode currents can be obtained using (2.24) if the common-mode currents are measured with a current probe. The current probe placed around both wires would give $2I_{mc}$. Relation (2.24) becomes:

$$\left|E_{C_{max}}\right| = 6.28\times10^{-7}\frac{I_{cur.probe}Lf}{R} \quad \text{V / m.} \tag{2.25}$$

Therefore accurate predictions of the radiated emissions from common-mode currents can be made if one measures the common mode currents with a current probe.

2.2 Methods for measuring the radiated field

2.2.1 Antenna-range measurements of radiation patterns

The ideal incident field for measuring the radiation characteristics of the test antenna is that of a uniform plane wave. In practice it is only possible to approximate such a field. Attempts to do this have led to the development of two basic types of ranges [3]:

- free-space ranges. This type of range is designed in such a manner that all the effects of the surroundings are suppressed to acceptable levels
- reflection ranges. This type of range is designed to judiciously use reflections in order to produce an approximated plane wave.

2.2.2 Measurement of power gain and directivity [3]

The power gain of an antenna, in a specified direction, is 4π times the ratio of the power radiated per unit solid angle in that direction to the net power accepted by the antenna from its generator. This quantity is an inherent property of the antenna and does not involve system losses arising from a mismatch of impedance or polarization. To determine the power transfer in a complete system, the antenna input impedance and the antenna polarization shall be measured and taken into account.

The directivity of an antenna in a specified direction is 4π times the ratio of the power radiated per unit solid angle in that direction to the total power radiated by the antenna. This term differs from power gain because it does not include antenna dissipation losses.

The directivity of a test antenna is obtained by integrating the measured far-field radiation patterns of the antenna over a closed spherical surface. If the antenna losses can

be determined by other means, then the power gain of the antenna can be determined from the directivity measurement

2.2.3 Distance aveaging method for antenna gain measurements in nonanechoic sites

Gain measurements are usually performed in a nonreflecting environment, for example, an anechoic chamber or an open test site. An anechoic chamber is quite expensive whereas an open test site requires a low-noise location. When measuring in a reflecting environment gating can actually eliminate the effect of reflections on the time-domain data issued either directly from measurement or from an inverse Fourier transform on frequency domain data [4], [5]. However, such a technique does not apply to narrow band antennas, as they normally yield time-domain responses longer than the delay of propagation by reflection or diffraction on the closest objects. Alternatively, the gain of a narrow band antenna can be evaluated from measurements inside a reverberation chamber [6] using a statistical model of the propagation.

The distance averaging method can be successfully used for measuring the antenna gain in a multipath site [7]. This method [7] derives from the two antenna method, assuming that one of the antennas has known radiation characteristics. The autors investigate how reflection and diffraction on commonly shaped objects impact on the normalized transfer function of a set of two omnidirectional antennas. A technique of averaging over the distance between antennas is applied, to reduce the effect of the multipath propagation. The measuring setup includes the antenna under test, a calibrated antenna, and a two-port vector network analyzer that measures the transfer scattering parameter. One of the antennas is placed at a fixed point and the other one is moved along a row or along several parallel rows. It comes out that averaging the magnitude of S_{21} weighted by the distance within a proper range results in a close approximation of that parameter for the free space, that is,

$$d_0 \cdot \left|S_{21,\text{ free space}}(d_0)\right| \cong d_0 \cdot \left|S_{21,\text{ approx}}(d_0)\right| = \frac{1}{N}\left|\sum_{n=1}^{N} d_k \cdot S_{21}(d_k) \cdot \exp(\mathrm{j}k_0 d_k)\right|, \tag{2.63}$$

where d_k is the distance between antennas, N is the number of measuring points, and d_0 is the reference distance (set at 1 m).

Let G_m be the gain of the measuring antenna. The gain of the antenna under test (AUT) can then be extracted,

$$G_{\text{AUT}} \cong \frac{{d_0}^2 \cdot \left|S_{21,\text{approx}}\right|^2}{G_{\text{m}}\left(1-\left|S_{22,\text{AUT}}\right|^2\right)} \cdot \left(\frac{4\pi}{\lambda}\right)^2 . \tag{2.64}$$

2.3 Methods for reducing the effect of common mode currents radiation

Most of the work treating the radiation from common mode currents at a symmetrical antenna input has focused on characterizing or properly designing a balun (Figure 2.10) [2], [8], rather than reducing that effect by post-processing.

a) Tub de ferită b) Balun din cablu coaxial

Figure 2.3 *Balun-uri utilizate pentru reducerea curenților de mod comun*

It is well known that when the antenna dimensions becomes comparable to those of ground plane (if any) and the feeding line, the common mode current becomes comparable in magnitude to the differential mode current drastically changing antenna properties [2]. For narrow band antennas different baluns are used to suppress common mode currents and prevent their propagation over feeding lines. In order to increase the common mode impedance of the antenna several designs of the feeding system have been numerically investigated. However, using a balun in a measuring setup not only increases the cost, but would also impinge on the global frequency response.

Some authors have proposed the replacement of the coaxial cable with optical fiber for eliminating the large distortion associated with the unwanted radiation from the feed line [9]. Electrically small antennas for wireless communications applications are prone to excite common mode currents on cables connected to them for measuring their performance. A miniature RF-optical transducer enables an optical fibre connection to the antenna, thereby eliminating the large distortion associated with the unwanted radiation from a coaxial cable. Results for measuring a small monopole antenna fed through coaxial cable and optical fibre in an anechoic chamber, are compared [9].

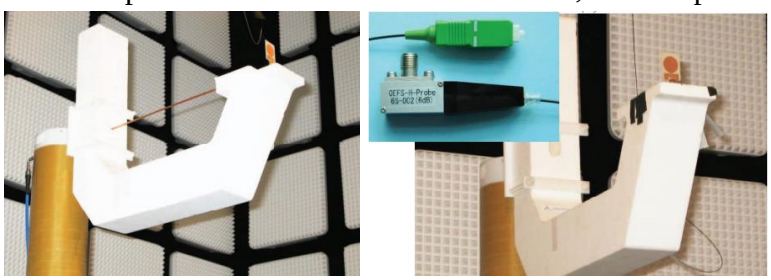

a) *b)*

Figure 2.4 *Experimental setup for radiation pattern measurement of a monopole antenna using: (a) coaxial cable; (b) optical fibre* [9]

This solution provides good results, but the cost of implementing such a measurement configuration is high.

Chapter 3

Measuring antennas for characterizing the radiation from common mode currents

When measuring the radiated field generated by common mode currents it is often necessary to separate the radiation sources (e.g., discrimination of the radiation generated by the common mode currents from the antenna radiation). Chapters 4 and 5 propose a number of source sepparation methods; depending on the concrete case studied, an antenna with linear polarization or with circular polarization is needed.

Among the linearly polarized antennas, the biconical antenna has the advantage of a very wide fractional frequency band. Among the circularly polarized antennas, the loop antenna is technologically easy to achieve and, even if it is a resonant antenna, its dispersive effect can be compensated by the subsequent processing of the measurement results.

3.1 Biconical antenna [10]

3.1.1 Radiated field

The electric field E_θ is related to the magnetic field H_ϕ by the intrinsic impedance, and we can write it as

$$E_\theta = \eta H_\phi = \eta \frac{H_0}{\sin\theta} \frac{\mathrm{e}^{-\mathrm{j}kr}}{r}. \tag{3.9}$$

The voltage produced between two corresponding points on the cones, a distance r from the origin, is found by

$$V(r) = \int_{\alpha/2}^{\pi-\alpha/2} \mathbf{E}\cdot \mathrm{d}\mathbf{l} = \int_{\alpha/2}^{\pi-\alpha/2} (\hat{\boldsymbol{a}}_\theta E_\theta)\bullet(\hat{\boldsymbol{a}}_\theta r \mathrm{d}\theta) = \int_{\alpha/2}^{\pi-\alpha/2} E_\theta r \mathrm{d}\theta. \tag{3.10}$$

The current on the surface of the cones, a distance r from the origin, can be expressed as

$$I(r) = \int_0^{2\pi} H_\phi r \sin\theta \mathrm{d}\phi = H_0 \mathrm{e}^{-\mathrm{j}kr} \int_0^{2\pi} \mathrm{d}\phi = 2\pi H_0 \mathrm{e}^{-\mathrm{j}kr}. \tag{3.11}$$

3.1.2 Input impedance

$$Z_c = \frac{V(r)}{I(r)} = \frac{\eta}{\pi} \ln\left[\operatorname{ctg}\frac{\alpha}{4}\right]. \tag{3.12}$$

Since the characteristic impedance is not a function of the radial distance r, it also represents the input impedance at the antenna feed terminals of the infinite structure.

3.2 Loop antenna

3.2.1 Small circular loop [10]

Magnetic field components:

$$H_r = \mathrm{j}\frac{ka^2 I_0 \cos\theta}{2r^2}\left[1+\frac{1}{\mathrm{j}kr}\right]\mathrm{e}^{-\mathrm{j}kr}, \tag{3.32a}$$

$$H_\theta = -\frac{(ka)^2 I_0 \sin\theta}{4r}\left[1+\frac{1}{\mathrm{j}kr}-\frac{1}{(kr)^2}\right]\mathrm{e}^{-\mathrm{j}kr}, \tag{3. 32b}$$

$$H_\phi = 0. \tag{3. 32c}$$

Electric field components:

$$E_r = E_\theta = 0, \tag{3.33a}$$

$$E_\phi = \eta\frac{(ka)^2 I_0 \sin\theta}{4r}\left[1+\frac{1}{\mathrm{j}kr}\right]\mathrm{e}^{-\mathrm{j}kr}. \tag{3.33b}$$

3.2.2 Circular loop of constant current [10]

The **E** și **H** fields can be written as

$$E_r \cong E_\theta = 0, \tag{3.68a}$$

$$E_\phi \cong \frac{ak\eta I_0 \mathrm{e}^{-\mathrm{j}kr}}{2r} J_1(ka\sin\theta), \tag{3.68b}$$

$$H_r \cong H_\phi = 0, \tag{3.68c}$$

$$H_\theta \cong -\frac{E_\phi}{\eta} = \frac{akI_0 \mathrm{e}^{-\mathrm{j}kr}}{2r} J_1(ka\sin\theta). \tag{3.68d}$$

Chapter 4

Polarization discrimination of the effects generated by the antenna and common mode currents

When both antenna and feeder have orthogonal polarizations, a separation between the field radiated by the antenna and the field originating from the feeder can be done by using a linearly polarized probe antenna.

This chapter describes a distance averaging approach that can be applied for discriminate the common mode currents effect on antenna feeders from the antenna radiation. By using the same measured data set, we present a comparison between the results processed by two alternative methods: our technique and time gating, respectively.

4.1 Methods for eliminating the effect of multiple propagation paths. Benchmarking

In Figure 4.1, we show the theoretical concepts for the distance averaging and time-gating methods, originally developed for antenna radiation measurements in a multipath site. We aim to assess the applicability of these two techniques for measuring the radiation from common mode currents on antenna feeders.

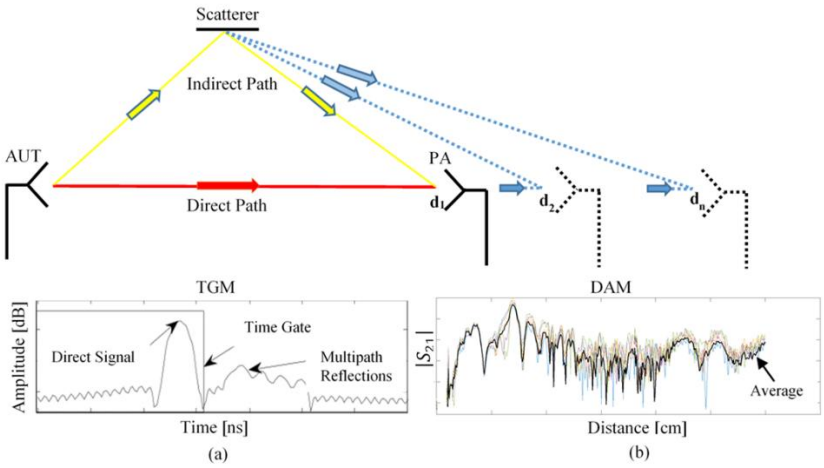

Figure 4.1 *Distance averaging vs time gating method*

4.1.1 Distance Averaging Method (DAM)

Antenna gain in a multipath site can be characterized by moving the antenna under test away from the probe antenna at different distances. By using DAM, one can reduce the effects of the indirect paths including reflection and diffraction on environing objects by measuring normalized transfer functions at different distances between the antenna under test (AUT) and the probe antenna (PA). The normalization of the transfer functions amounts to the compensation of the propagation effect as it would be in the free space, in terms of attenuation and delay [12].

The average transfer function can be computed from the transfer functions measured at each distance d_k between antennas,

$$\bar{S}_{21} = \sum_{n=1}^{N} \frac{d_k}{d_0} \exp\left(\mathrm{j}k_0 d_k\right) S_{21}^{d_k}, \tag{4.1}$$

where d_0 is the reference distance (set at 1 m) and k_0 is the free space wavenumber.

4.1.2 Time-Gating Method (TGM)

The effect of the propagation over indirect paths can be reduced in the time-domain by simply gating out the response over the direct path (Figure 4.1a), provided that it induces the shortest time delay. In order to accurately extract the AUT gain the time gate should be properly chosen [13]. The upper limit of the time- domain window should be chosen such as

$$t_w = \frac{d}{c_0}, \tag{4.2}$$

where d is the direct pathlength and t_w is the time-domain window length.

When measuring the radiation from common mode currents in a multipath site a time-domain window length longer than the direct path propagation delay might be needed, as the response corresponding to radiation of the feeder is often longer.

In that case, the time gate upper limit should be correlated to the shortest indirect path, $r_{i,min}$ i.e.,

$$t_w = \frac{r_{i,\min}}{c_0}. \tag{4.4}$$

4.2 Experimental validation

In order to validate our approach we measured a log-periodic dipole array; as a probe we employed a calibrated, biconical dipole. A vector network analyzer was used for measuring the scattering parameters of the two-port system; the setup is shown in Figure 4.3. The measurements were performed within a multipath site (an ordinary room inside a building).

The measurements were performed at distances between 20 and 40 cm between antennas. The distance increment was 5 cm.

Figure 4.2 *Measuring setup for experimental validation*

In Figure 4.4, we show the normalized transfer functions, measured at each of the 5 distances between the log-period dipole array and the antenna probe. On the same diagram we give the average figure resulting from (4.1).

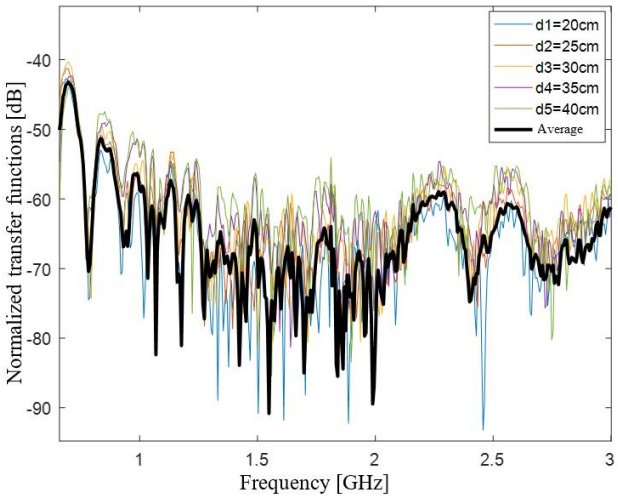

Figure 4.3 *Normalized transfer functions and average figure*

The time-domain response $s_{21}(t)$ and its time gate is shown in Figure 4.5. The closest object in the measuring environment was at 3m away from the measuring setup. That is, a time gate length approximatively 25ns should be used.

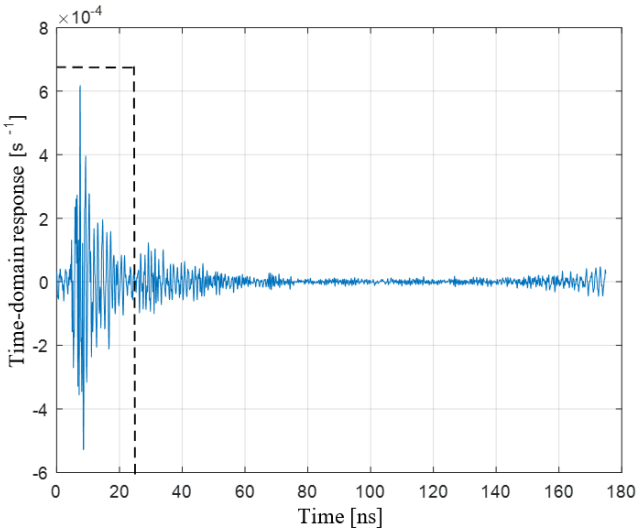

Figure 4.4 *Time-doman response and time gate*

In Figure 4.7 and Figure 4.8, we show a comparison between the results provided by DAM and TGM, in terms of normalized transfer functions and gain of the feeder, as a radiator.

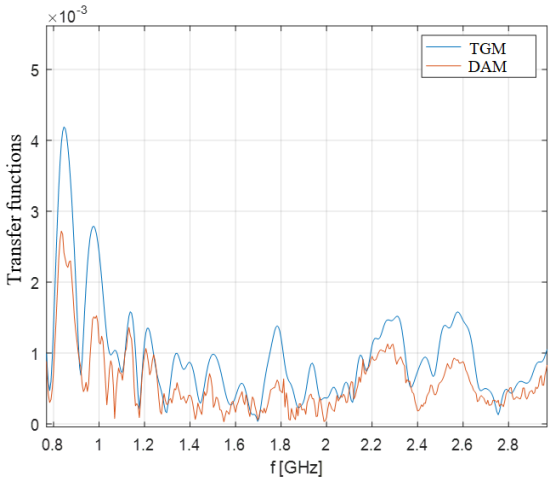

Figure 4.6 *Transfer functions after TGM and DAM*

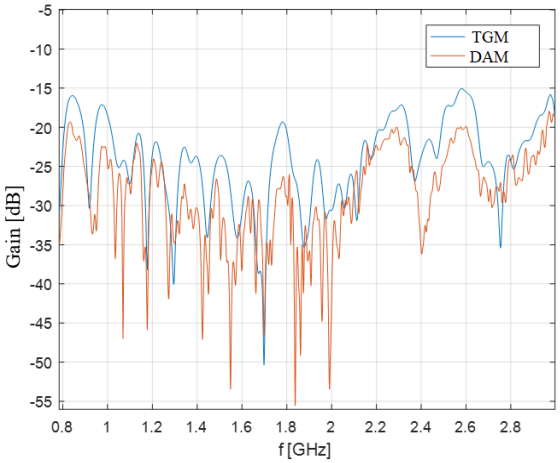

Figure 4.6 *Gain of the feeder as a radiator*

In this chapter, we showed that a distance averaging approach can be used for measuring the radiation from common mode currents on a coaxial line feeding a symmetrical antenna. The discrepancies are due to the fact that the accuracy of time gating method may depend on the relation between length of the impulse response of the radiating feeder, and the distribution of the scatterers within the measuring site. Part of the differences between the results provided by the two methods may originate from the field radiated by the log-periodic antenna, since the environing objects can rotate the polarization of the incident field. The field radiated by the log-periodic antenna is much stronger than the field generated by the common mode currents; however, the effect of the former is dramatically reduced by the distance averaging approach, since it follows an indirect path.

Chapter 5

Discrimmination of the field generated by common mode currents from the field generated by the antenna using the distance averaging method

This chapter proposes an alternative method for separating the effects of the two sources, starting from the variability of the common mode current distribution.

5.1 The principle of the method

For each type of antenna analyzed, two measurement configurations will be defined (Figure 5.1):

- for the first configuration, the PA will measure the field generated by the AUT and the field generated by the common mode currents on the feeder as well;
- for the second configuration, the PA will measure only the field yield by the AUT.

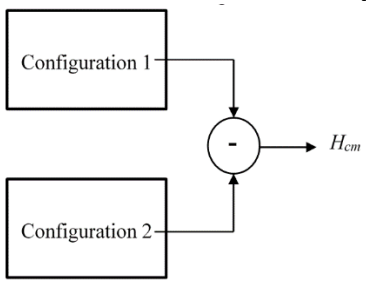

Figure 5.1 *The principle of separation of common mode currents radiation*

Starting from this configurations, we developed a differential approach for evaluating the magnetic field generated by the common mode currents on an antenna feeder.

5.2 Case study: symmetrical antennas

5.2.1 Impact reduction of common mode currents on antenna feeders in radiation measurements

When measuring the field radiated by symmetrical antennas, the distance averaging technique can be apply in order to reduce the effect of the common mode currents. For experimental validation [16], [17]: (1) We propose two different approaches for this technique, depending on the number of the symmetry degrees of the antenna under test; (2) we present a distance averaging method to extract the effective area of the loop antenna that we used as a probe; and (3) we develop a differential approach for evaluating the magnetic field generated by the common mode currents on an antenna feeder.

We considered a typical two-antenna measuring system consisting of a probe antenna (PA) and an antenna under test (AUT), respectively. As an AUT, we successively used two types of symmetrical radiators fed through coaxial cables: a two-symmetry degrees antenna (i.e., a dipole) and a one-symmetry degree antenna (i.e., a log-periodic dipole array). As a PA, we took a small, square loop antenna.

We designated as the "cable side" the field points in a direction orthogonal to the antenna, along the feed line. The "antenna side" will include field points in the same direction, but on the cable free side. The field on the "antenna side" is entirely due to the radiation of the AUT, conversely, on the "cable side", the field is due both to the radiation of the AUT and the cable.

We propose two different measuring methodologies depending on the number of symmetry degrees of the antenna under test.

➢ When using a simple wire dipole, measurements will be performed by placing the probe on each side of the antenna (Figure 5.2).

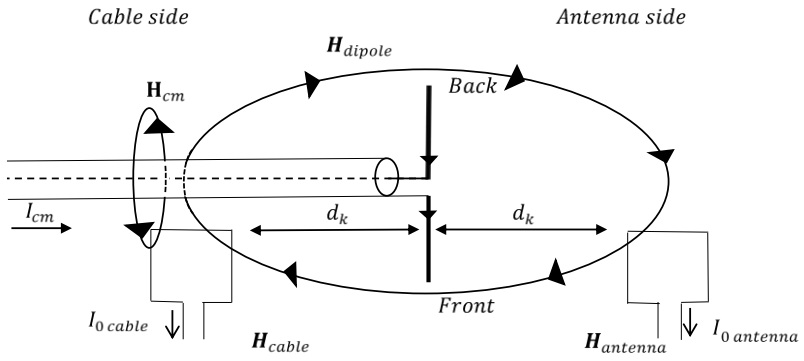

Figure 5.2 *Measuring methodology for a dipole antenna.*

➢ When using the log-periodic dipole array as an antenna under test, measurements are performed by successively placing the coaxial cable on both sides of the feed point (Figure 5.3).

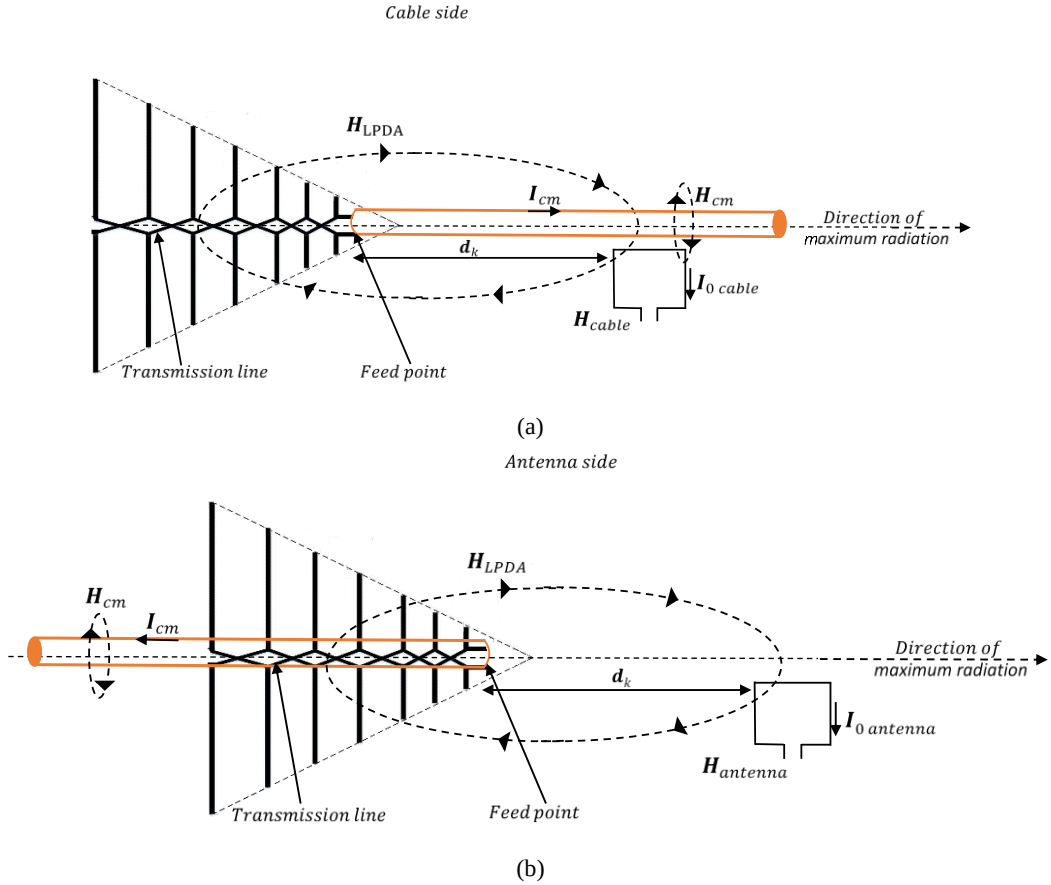

Figure 5.3 *Measuring methodology for a log-periodic dipole array: "cable side" (a) and "antenna side" (b).*

For each type of AUT, the effect of the common mode current on the coaxial line can be assessed by subtracting the field measured at the same distance with the probe placed on the "cable side" and on the "antenna side", respectively. Such measurements are performed at several distances between the antenna under test and the probe, in order to apply the distance averaging approach [7].

Referring to Figures 5.2 and 5.3, the magnetic field measured by the loop on the "cable side" and "antenna side" can be expressed as

$$H_{cable} = H_{cm} + H_{dipole/LPDA}, \tag{5.1}$$

where H_{cm} is the magnetic field component generated by the common mode currents and $H_{dipole/LPDA}$ is the field component generated by the antenna.

The contribution of the common mode current to the magnetic field can be found as

$$H_{cm} = H_{cable} - H_{antenna}, \tag{5.2}$$

where

$$H_{antenna} = H_{dipole/LPDA}. \tag{5.3}$$

When transfer functions are measured at *N* different distances an average can be computed over that data set by compensating the effects of the multipath propagation. As the field corresponding to indirect propagation paths, common mode currents have also a distance variant distribution. The application of the distance averaging (Figure 5.5 for dipole antenna and Figure 5.6 for log-periodic dipole array) might therefore significantly reduce the impact of the common mode current on antenna radiation measurements.

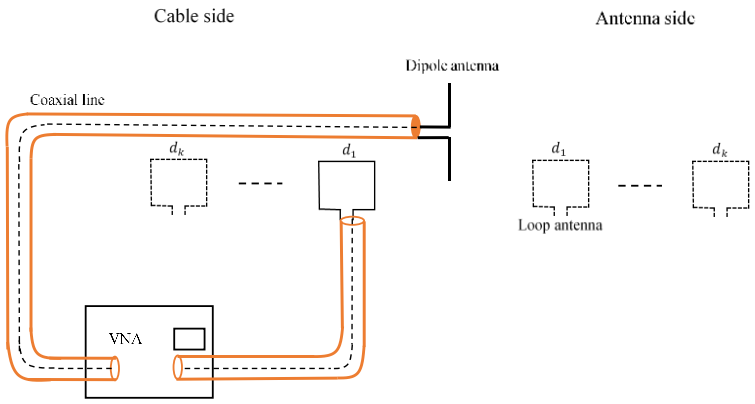

Figure 5.4 *Distance averaging technique applied for reducing the effect of the common mode current on dipole antenna radiation measurements.*

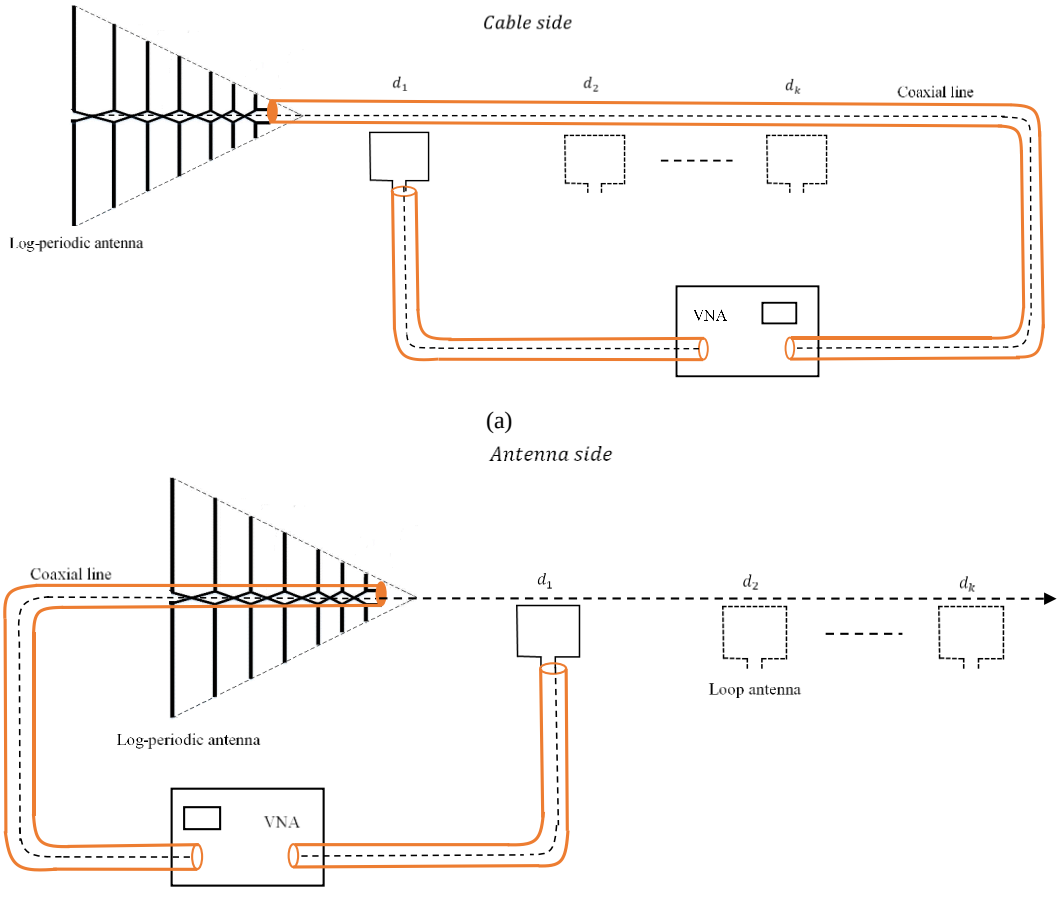

Figure 5.5 *Distance averaging technique applied for reducing the effect of the common mode current on LPDA radiation measurements: cable side (a) and antenna side (b).*

The average transfer function can be computed from the transfer functions measured at each distance d_k between antennas,

$$\bar{S}_{21\,cm} = \sum_{k=1}^{N} d_k \exp\left(\mathrm{j}k_0 d_k\right) S_{21\,cm}^{d_k}, \tag{5.11}$$

where k_0 is the free space wavenumber and d_0 is the reference distance (set at 1 m).

The effect of the common mode currents should be reduced for cable side measurements and therefore corrected figures should be calculated,

$$\bar{S}_{21\,mc.cor} = \sum_{k=1}^{N} \frac{d_k}{d_0} \exp\left(\mathrm{j}k_0 d_k\right) S_{21\,mc}^{d_k}. \tag{5.18}$$

$$H_{cablu.cor}^{d_k} = d_k \exp\left(-\mathrm{j}k_0 d_k\right) \bar{H}_{cablu}. \tag{5.19}$$

Relation (5.19) gives the field value at a given distance by simply multiplying the result by that distance, provided that the average figure corresponds to a distance of 1m between antennas.

5.2.2 Probe antenna calibration using the distance averaging method

One of the AUTs (i.e., the LPDA) has previously been calibrated inside a professional, compact range in an “antenna side” setup (Figure 5.8).

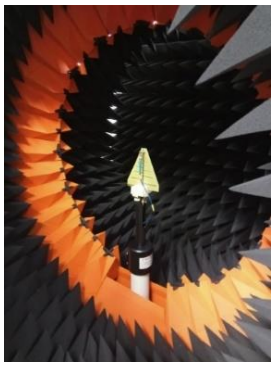

Figure 5.6 *LPDA calibration.*

As a result, that AUT could itself be used as a probe for calibrating the loop when the LPDA is in an “antenna side” configuration. Furthermore, the loop calibrated as described previously will be able to measure the radiation of any other configuration (e.g., with the LPDA) in a “cable side” setup, or the dipole in an “antenna side” and “cable side” setup.

Since the loop is used as a probe (receiving) antenna, one should characterize it through its effective area, rather than its gain, that is,

$$A_e = \frac{4\pi d^2}{G_t} \frac{R_0}{R_{a2}} \frac{\left|S_{21}\right|^2}{\left|1-S_{22}\right|^2 \left(1-\left|S_{11}\right|^2\right)}. \tag{5.24}$$

In order to accurately evaluate the effective area of the probe antenna in a multipath environment, we used the distance averaging method. The setup in shown in Figure 5.10.

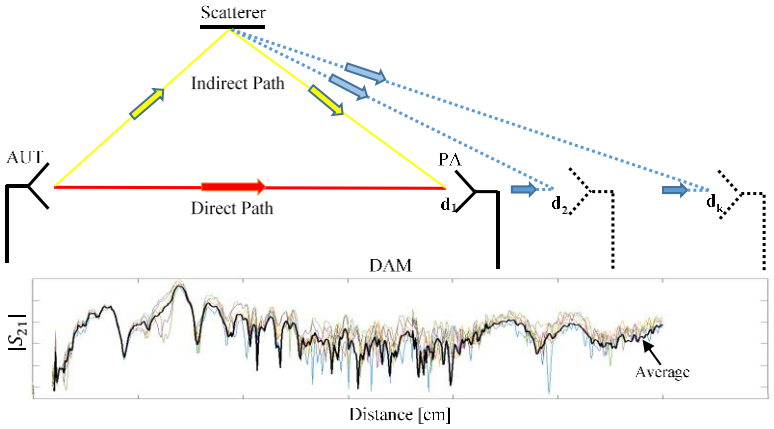

Figure 5.7 *Distance averaging method.*

5.2.3 Experimental validation

In order to validate our approach, we measured a dipole and a LPDA, respectively, by using a square loop probe. The dipole was resonating around 1.2 GHz and had a total length of 9 cm. The LPDA was designed for the frequency range 800 MHz−3 GHz and was 13 × 13 cm in size. As a probe, we used a square loop with a side length of 2 cm. The measurements were performed in a non-anechoic environment (a regular room inside a building).

Since the LPDA has been calibrated inside a compact range in an “antenna side” type configuration, we firstly extracted the effective area of the loop when placed in the same configuration. We used the distance averaging approach as the measurements were performed in an environment with multiple propagation paths.

Figure 5.12 shows the normalized transfer functions of the antenna system measured at eight different distances ranging between 25 and 60 cm, and the average transfer function.

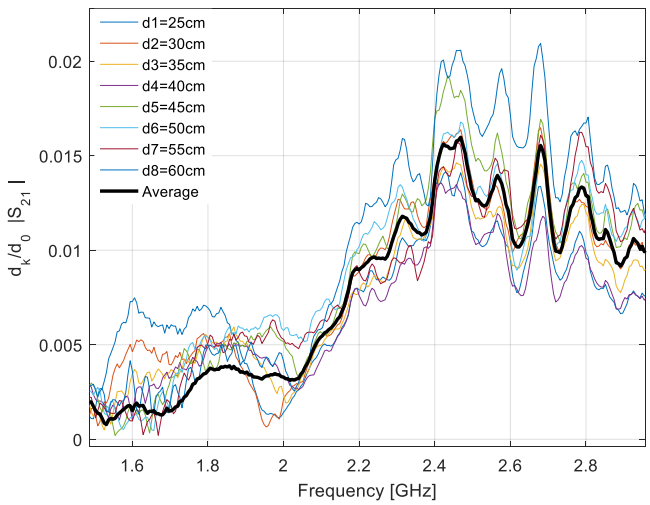

Figure 5.8 *Normalized transfer functions and the average figure.*

The effective area of the loop as a function of frequency is given in Figure 5.13:

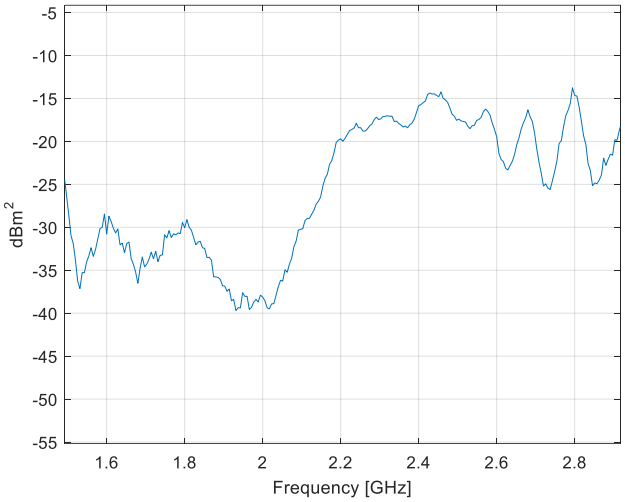

Figure 5.9 *Effective area of the loop probe.*

Once the loop probe calibrated, we assessed the effect of the common mode currents by measuring the transfer functions both on the "antenna side" and "cable side" for each AUT. The setup for each AUT is presented in Figure 5.14 and Figure 5.15, respectively.

(a) (b)

Figure 5.10 *Measuring setup for a dipole antenna: "cable side" (a) and "antenna side" (b)*

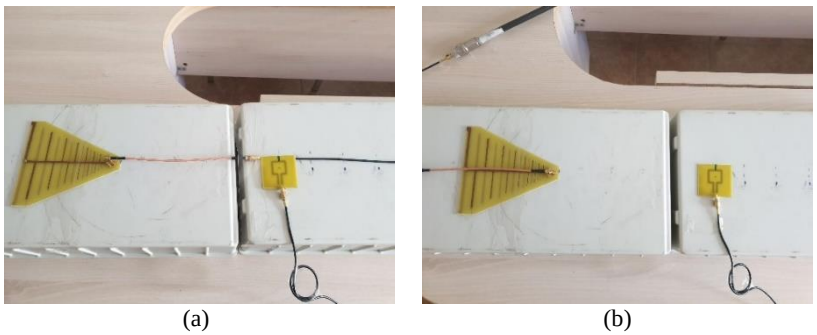

(a) (b)

Figure 5.11 *Measuring setup for a LPDA: "cable side" (a) and "antenna side" (b)*

For the dipole antenna the measurements on the "cable" and "antenna side" were performed at distances between antennas ranging from 5 to 40 cm with a distance

increment of 5 cm. For the LPDA the distance to the probe ranged between 25 and 60 cm with the same increment. All the distances correspond at least to the Fresnel zone [18]. The measurements on both antennas were performed between 1.5−3GHz, a frequency range where the loop has a good radiation efficiency. The effect of the impedance mismatch at the probe output was corrected on the measured data. The magnetic field generated by the common mode currents can be evaluated by subtracting the results measured on the "antenna side" from those measured on the "cable side" (Figure 5.16).

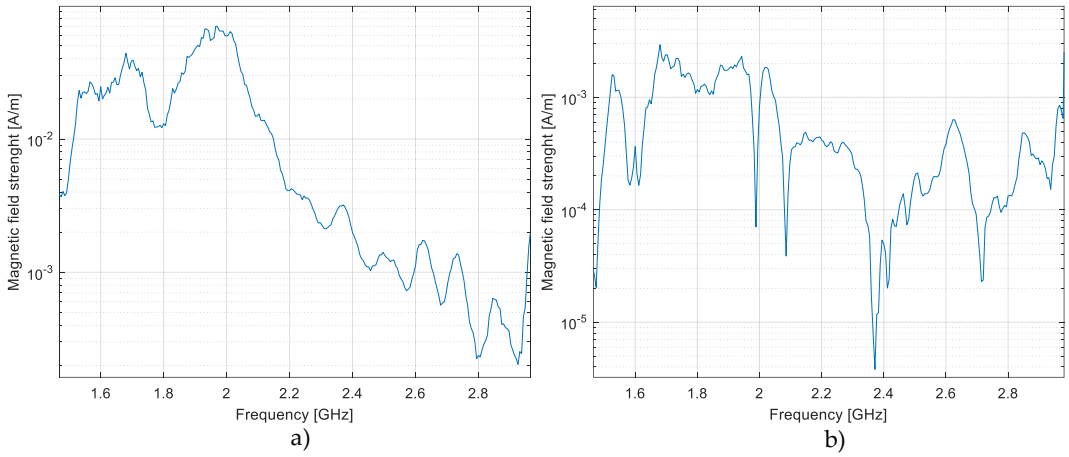

Figure 5.12 *Magnetic field generated by common mode currents: dipole (a) and LPDA (b)*

In Figure 5.17, we show the contribution of the common mode current to the output current, measured at each of the eight distances between the loop and AUT. On the same diagram we give the average figure.

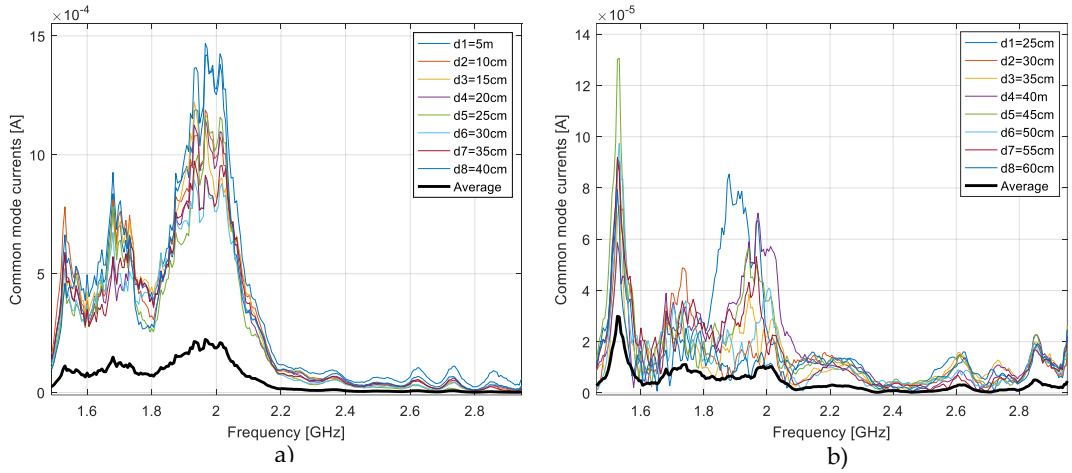

Figure 5.13 *Contribution of the common mode current to the output current versus distance averaged figure: dipole (a) and LPDA (b)*

As Figure 5.17 shows the common mode contribution to the output current can be dramatically diminished by applying the distance averaging technique.

In Figure 5.18, we give the variation of the corrected, magnetic field strength as a function of distance and frequency.

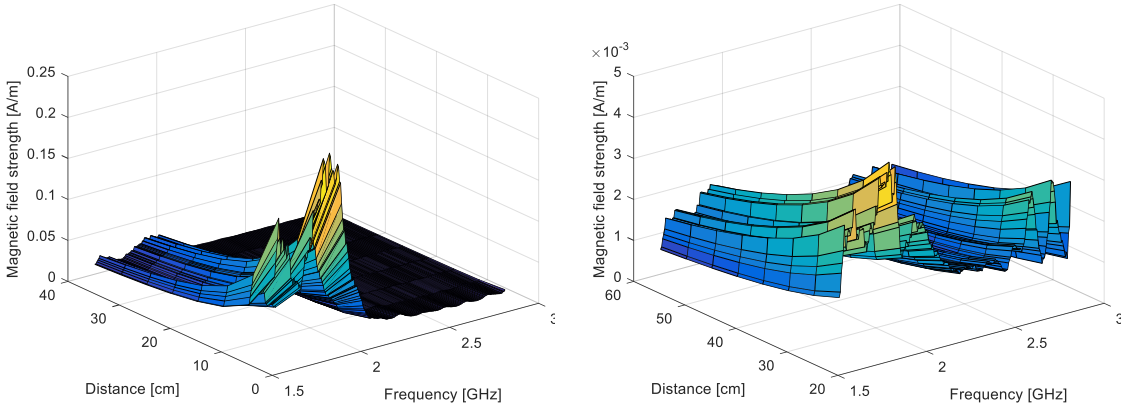

(a) (b)

Figure 5.14 *Magnetic field measured on the "cable side" after correction, as a function of distance and frequency: dipole (a) and LPDA (b).*

Figure 5.19 shows a comparison between the magnetic field measured on the "cable side" at 40 cm, with and without correction of the common mode current effect, and the magnetic field on the "antenna side" at the same distance.

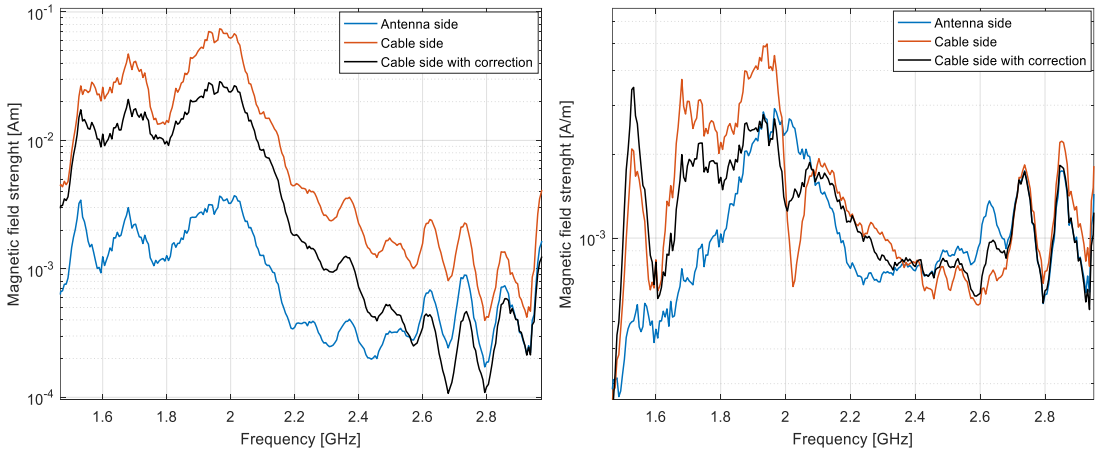

a) *b)*

Figure 5.15 *Magnetic field measured for "antenna side" and for "cable side", with and without correction: dipole antenna (a) and LPDA (b).*

It appears that by applying our distance averaging technique, the corrected magnetic field magnitude on the "cable side" got closer to the magnetic field strength measured on the "antenna side". We defined a root mean square error by taking the field strength on the cable free side as a reference. The error decreased from 71% down to 29% for the dipole and from 6.2% down to 3.1% for the LPDA.

5.3 Case study: asymmetrical antennas

5.3.1 Discrimination of radiation sources effects

We propose a new strategy to apply the distance averaging method to discriminate the radiation generated by the coaxial cable feeding a small monopole antenna from the antenna radiation.

Such an effect discrimination is necessary in order to correct radiation pattern measurement in a minor radiation direction e.g., below the ground plane of a monopole antenna.

The method was validated by measuring a monopole antenna with a small square loop as a probe.

We designate as "*xOy* polarization" setup a measuring configuration with the loop placed in the *xOy* plane i.e., in the same plane with the feeder (Figure 5.20). The loop will measure the field generated by the antenna and the field generated by the common mode currents on the feeder as well.

It should be noted that the field generated by the antenna on the backside of the ground plane is mostly due to the ground current distribution, but the radiating rod of the monopole may also contribute through diffraction on the ground edges.

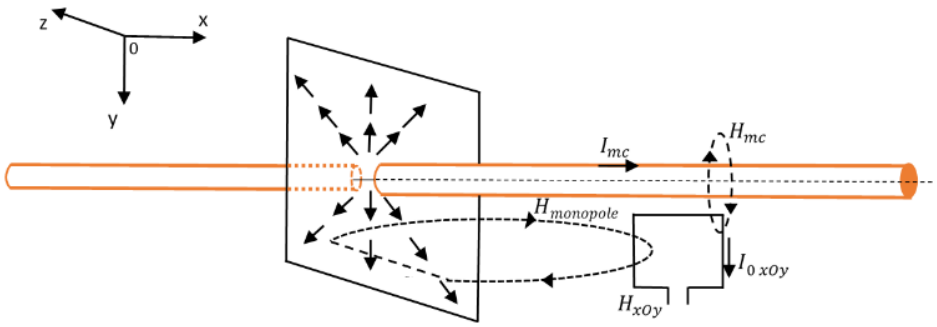

Figure 5.16 *Magnetic field components through the PA for xOy polarization measurements*

The " *yOz* polarization" designates the measurements with the loop placed in two different configurations that will allow to measure only the field yield by the antenna (Figure 5.21). To achieve this, two measurement possibilities are proposed:

a) the loop will be placed in the *yOz* plane i.e., parallel to the ground plane (Figure 5.21a). In this case, the loop will solely measure the field yield by the antenna, since the magnetic field generated by the common mode currents are parallel to the PA.

b) the coaxial cable will be moved in symmetrical positions located on either side of its initial direction and the measured values will be averaged so that the contribution of the common mode currents will be substantially reduced (Figure 5.21b). For this measurement configuration only the cable will be moved in different positions, while the loop will have the same orientation as in the case of the "xOy polarization" configuration. For this case, the radiation contribution of the currents will vary depending on the position of the cable, while the radiation contribution of the antenna will remain unchanged.

Therefore, if an average is calculated over this set of values, the variable contribution of the common mode currents tends to cancel out.

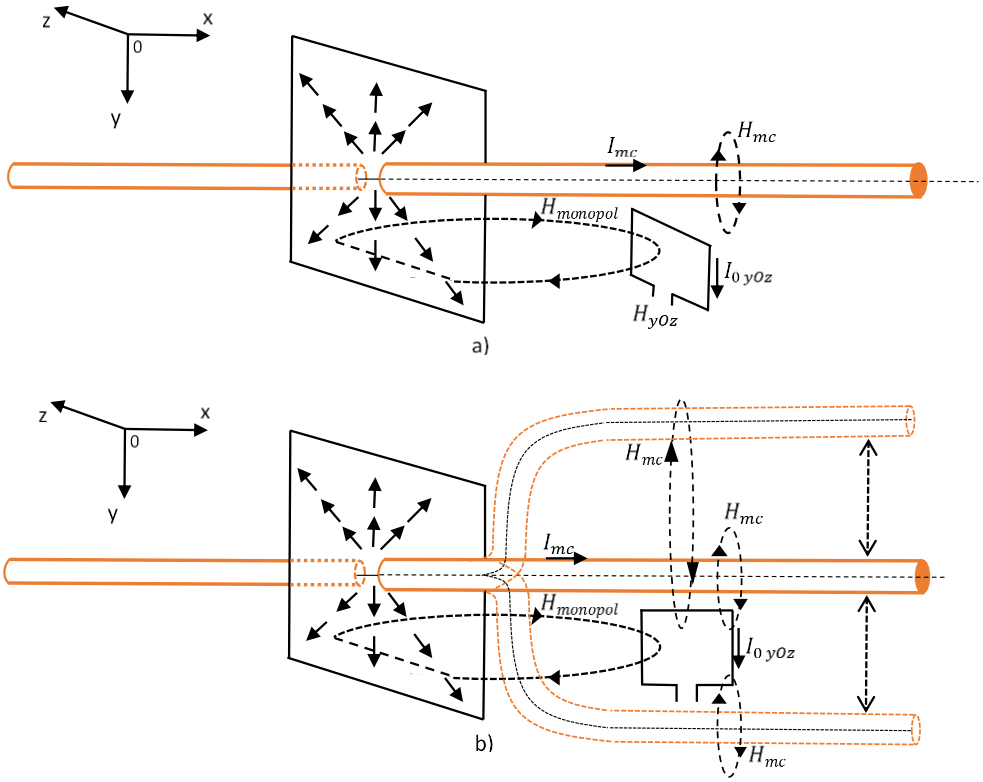

Figure 5.17 *Magnetic field components through the PA for yOz polarization measurements: a) loop perpendicular to the cable and b) cable movement*

Since common mode current distributions vary with the distance in a similar way as the radiated field in a multipath environment we propose to apply the distance averaging technique in order to reduce the effect of the common mode currents for the *xOy* polarization (Figure 5.22) and for the *yOz* polarization when mooving the cable (Figure 5.23b). We also apply that technique for the yOz polarization (Figure 5.23) in order to remove the effect of the multipath propagation; moreover, the reduction of the multipath propagation effect also occurs as a side benefit of the method for the xOy polarzation (Figure 5.22).

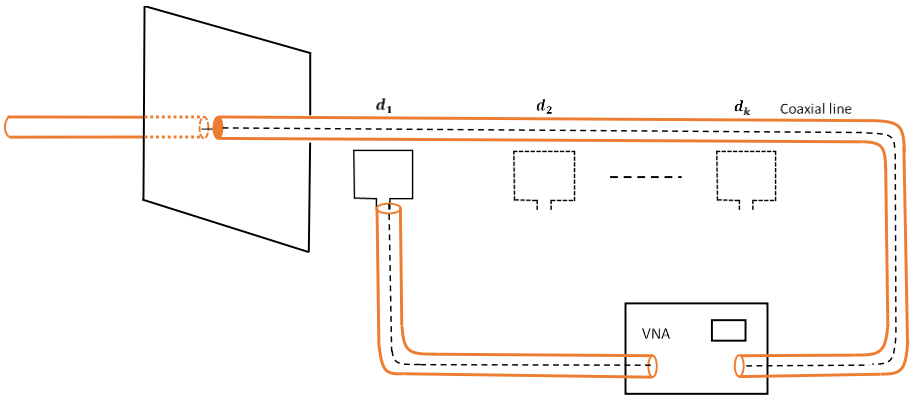

Figure 5.18 *Distance averaging method for xOy polarization*

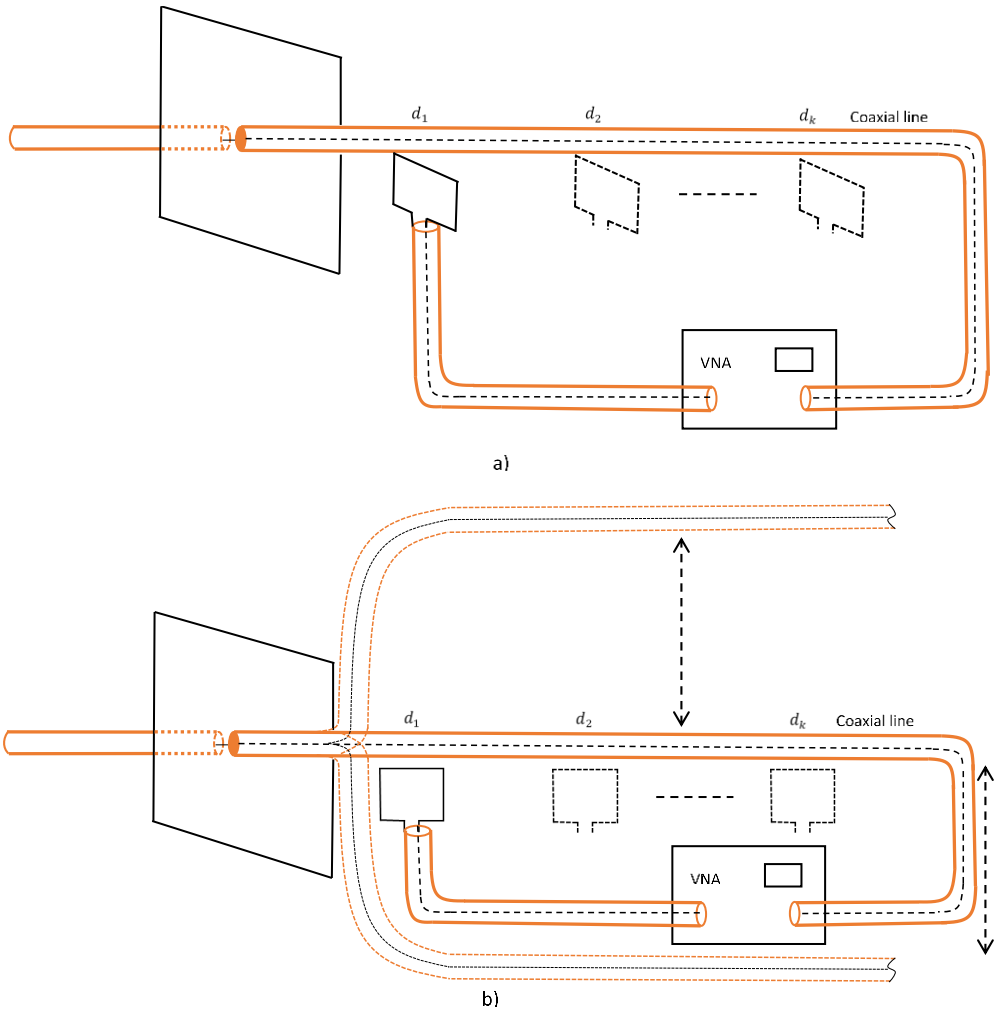

Figure 5.19 *Distance averaging method for xOy polarization: a) loop perpendicular to the cable and b) cable movement*

As the effect of the common mode currents should be reduced for the *xOy* polarization measurements, corrected figures for the magnetic field can be derived for any measuring position, based on the average field (assessed at 1m),

$$H_{xOy.cor}^{d_k} = d_k \exp\left(-\mathrm{j}k_0 d_k\right) \bar{H}_{xOy}. \tag{5.35}$$

5.3.2 Experimental validation

The measuring setup is illustrated in Figure 5.25. The antenna under test was a monopole with a 25cm high radiating rod, and a ground plane side length of 10cm. The probe was a calibrated square loop with a side length of 2cm. Both antennas were connected to a vector network analyzer (VNA) through 50Ω coaxial cables. The measurements were performed by using a VNA in a non-anechoic environment. The loop was placed at seven different distances between the AUT and the PA for each measuring configuration, *xOy* and *yOz*.

Measurements were performed for distances between 10 and 40cm with a pitch of 5cm, for both measurement configurations and at frequencies between 1.5GHz and 3GHz.

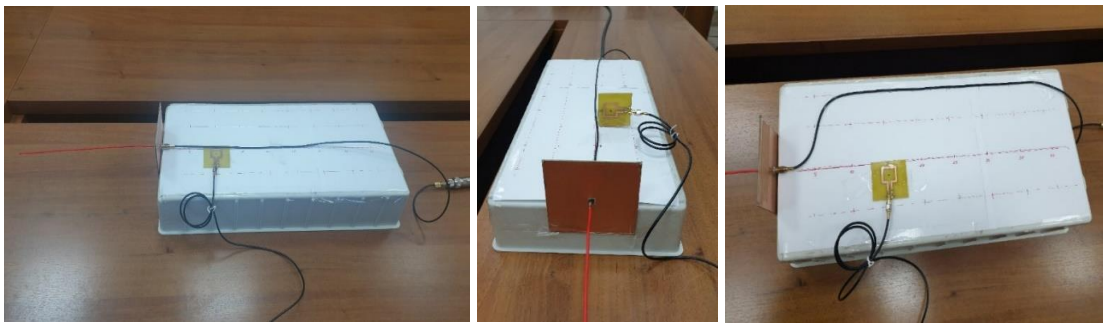

a) *b)* *c)*

Figure 5.25 *Measuring setup: (a) xOy polarization, (b) yOz polarization- loop perpendicular to the cable and (c) yOz polarization- cable movement*

Figure 5.26 depicts the contribution of the common mode current to the output current, measured at each of the seven distances between the loop and AUT. On the same diagram we give the average figure.

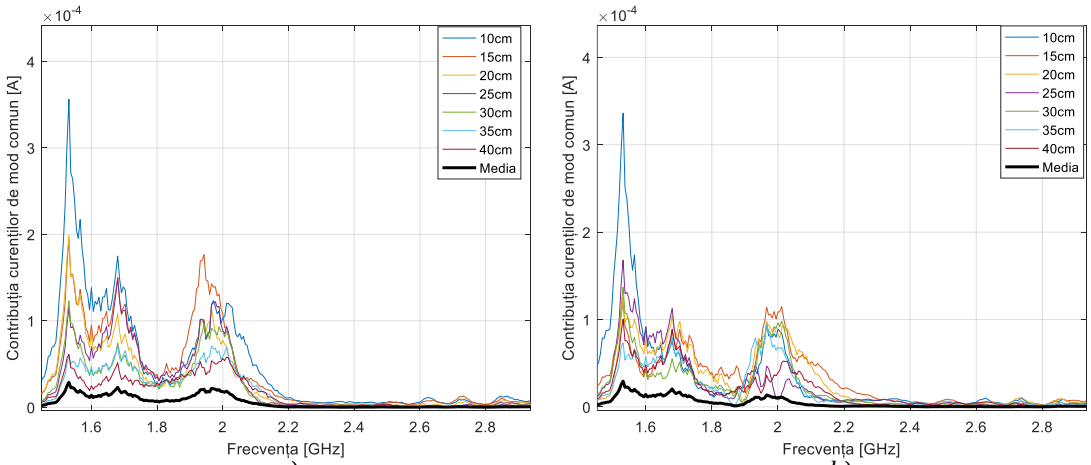

a) *b)*

Figure 5.26 *Contribution of the common mode current to the output current at different distances, and average figure: yOz polarization- loop perpendicular to the cable (a), yOz polarization- cable movement (b)*

It can be seen that the distance averaging method significantly reduces the contribution of the common mode current. Thus, it is demonstrated that the two configurations chosen for the *yOz* polarization, lead to very close results.

The magnetic field generated by the common mode currents can be computed by subtracting the yOz polarization result from the xOy polarization results (Figure 5.27). It should be noted that such a determination is possible without considering any phase difference between the two terms, given that the distance averaging method brings the phase centers of both radiation sources, to the origin.

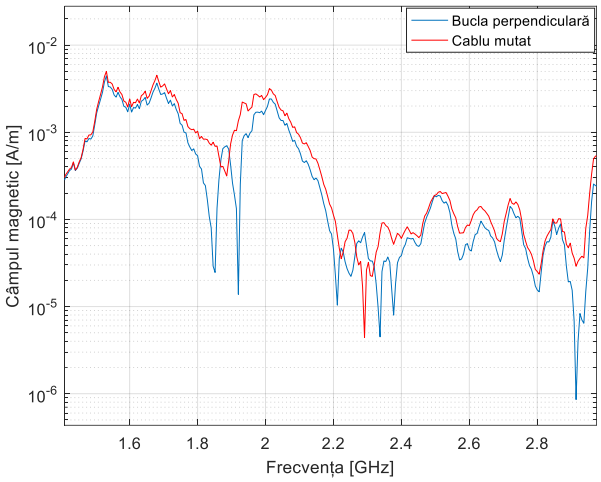

Figure 5.27 *Magnetic field generated by common mode currents measured at a distance of 40cm between the AUT and the PA.*

In Figure 5.29 we show a comparison between the magnetic field measured for *xOy* polarization, *yOz* polarization, and the corrected field for xOy polarization. The distance between the AUT and PA was set at 40cm.

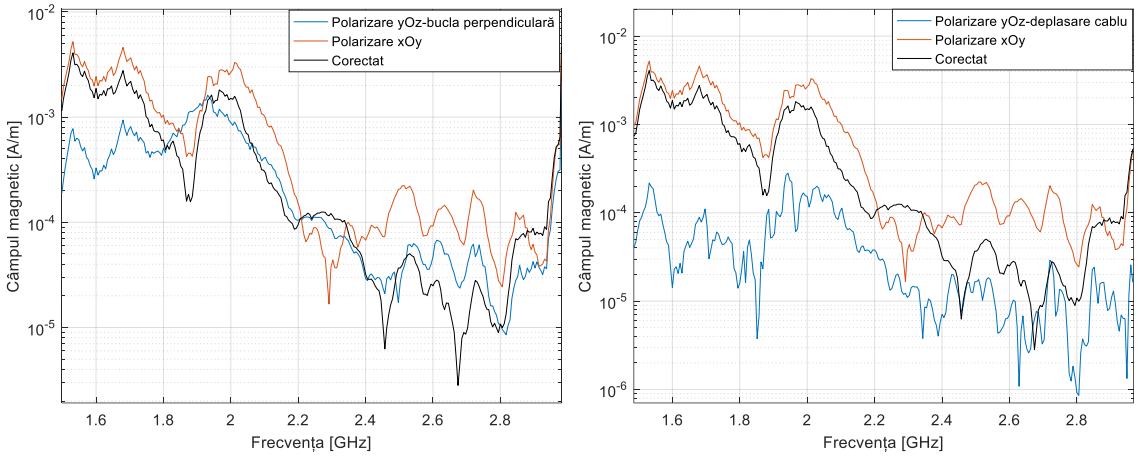

a) *b)*

Figure 5.29 *Magnetic field measured for xOy polarization, yOz polarization- loop perpendicular to the cable (a), yOz polarization- cable movement (b), and the corrected field for xOy polarization*

It can be seen that the value of the corrected field obtained for the *xOy* polarization configuration tends to be closer to the value of the field obtained for the *yOz* polarization configuration. The best results are obtained for frequencies higher than 2GHz, i.e., frequencies for which the efficiency of the loop is maximum.

We also computed a root mean square error for *xOy* polarization by taking as a reference the field measured for *yOz* polarization. The root mean square error decreases from 21% down to 7%, so the error was roughly reduced by a factor of 3.

Chapter 6

Conclusion

6.1 Results

In this work, two directions of research for the separation of the effects of radiation generated by common currents when measuring antenna gain in a multipath propagation environment, were investigated.

The first direction is presented in chapter 4 and consists in the polarization separation of the two radiation sources (the antenna and the cable whose external conductor is crossed by common currents). An ultra-wideband linear polarization antenna (a biconical dipole) was used for this purpose.

In order to eliminate the effects of the multipath propagation, the distance averaging method was applied for the first time in a secondary direction of radiation.

The field radiated by the AUT is much stronger than the field generated by the common mode currents; however, the effect of the former is dramatically reduced by the distance averaging approach, since it follows an indirect path. It has been shown that the distance averaging method works with high precision even in conditions of reflection, diffraction and rotation on obstacles of the polarization of the field produced by the antenna in the main direction of radiation.

The experimental validation was performed by measuring a log-periodic dipole array fed through a coaxial line. The time gating method was chosen as a reference for evaluating the results, in which the length of the time window was established in correlation with the shortest indirect propagation path, in order to compensate the dispersive character of the feeder, as a radiator.

The second research direction in order to discriminate the effects of the two radiation sources is presented in chapter 5 and consists in a separate measurement of the field in two configurations, using a dual polarization antenna (loop antenna). In one of the two configurations the induced current in the loop is proportional to the field generated by the whole assembly (antenna and feeder), and in the other configuration the induced current is proportional only to the field produced by the antenna. Three strategies have been developed to allow such measurements in the following cases: a one-symmetry degree antenna (i.e., a log-periodic dipole array), a two-symmetry degrees antenna (i.e., a dipole) and an asymmetrical antenna (i.e., a monopole).

We proposed a differential approach for evaluating the magnetic field generated by the common mode currents on an antenna feeder.

In order to extract the effective area of the loop probe, we applied a distance averaging technique derived from an approach originally developed for antenna gain measurements in a multipath site.

We also developed a distance averaging approach for correcting the field radiated by the AUT fed through a coaxial line, with the effect of the common mode current. The common mode current has a distance variant distribution and therefore, its effect on the field measured aside the feeder can be diminished by averaging the results acquired at different distances between the probe and the antenna under test. By applying the proposed technique, a magnetic field value corresponding to a reference distance of 1 m was first derived; the actual corrected field value was then found by multiplying the result by the distance and the corresponding phase factor.

The root mean square error on the measured field magnitude was reduced at least by a factor of two for all three antennas under test.

6.2 Original contributions

1. The distance averaging method was applied for the first time in a secondary direction of radiation in order to separate in polarization the radiated fields from the antenna and the coaxial cable, respectively [LO2].

2. A new approach for the time gating method in which the length of the time window was established in correlation with the shortest indirect propagation path, in order to compensate the dispersive character of the feeder, as a radiator [LO2].

3. A novel technique that can be applied in a multipath propagation environment in order to discriminate the effects of the two radiation sources, consisting in a separate measurement of the field in two configurations. In one of the two configurations the induced current in the loop is proportional to the field generated by the whole assembly (antenna and feeder), and in the other configuration the induced current is proportional only to the field produced by the antenna [LO1], [LO3],[LO4], [LO6].

4. In order to extract the effective area of the loop probe, we applied a distance averaging technique derived from an approach originally developed for antenna gain measurements in a multipath site [LO1], [LO5].

5. A new strategy for placing the PA to separate the radiated fields from a one-symmetry degree antenna and the coaxial cable, respectively [LO1], [LO6].

6. A new strategy for placing the PA to separate the radiated fields from a two-symmetry degree antenna and the coaxial cable, respectively [LO1], [LO3].

7. A new strategy for placing the PA to separate the radiated fields from an asymmetrical antenna and the coaxial cable, respectively [LO4].

8. A differential approach for evaluating the magnetic field generated by the common mode currents on an antenna feeder [LO1], [LO3], [LO4], [LO6].

9. A new method for impact reduction of common mode currents on antenna feeders in radiation measurements. This method can be applied dueto the distance variability of the common mode currents along the feeder [LO1], [LO3], [LO4], [LO6].

6.3 Publications

[LO1] **A. Constantin**, R.D. Tamas**,** *Evaluation and Impact Reduction of Common Mode Currents on Antenna Feeders in Radiation Measurements*, **Sensors**, vol. 20, no. 14, Art. no. 14, Jan. 2020, doi: 10.3390/s20143893**. - *indexat WoS, Q1*.**

[LO2] **A. Constantin**, R.D. Tamas**,** L. Anchidin, *A Distance Averaging Approach for Measuring the Radiation from Common Mode Currents on Antenna Feeders*, **in Proceedings of the IEEE International Workshop on Antenna Technology,** București, România, pp.1-4, doi: 10.1109/iWAT48004.2020.1570612231, 25-28 Feb. 2020- ***indexat WoS*** și ***IEEE Xplore***.

[LO3] **A. Constantin**, R.D. Tamas**,** L. Anchidin, G. Caruntu, *A New Method to Reduce the Impact of the Common Mode Currents for Field Measurements on Symmetrical Antennas*, **in Proceedings of the IEEE International Workshop on Antenna Technology,** Miami, Florida, pp.87-90, doi: 10.1109/IWAT.2019.8730606, Mar. 2019 - ***indexat WoS*** și ***IEEE Xplore***.

[LO4] **A. Constantin**, R.D. Tamas**,** *Radiation from Common Mode Currents on Coaxial Lines Feeding Small Monopole Antennas*, **in Proceedings of the IEEE Telecoms Conference (ConfTELE),** Leiria, Portugalia, 11-12 Feb. 2021- ***indexat WoS*** și ***IEEE Xplore.***

[LO5] **A. Constantin**, R.D. Tamas**,** *Loop probe calibration for radiation measurements from common mode currents*, **in Proceedings of the IEEE International Symposium on Signals, Circuits and Systems,** Iași, România, pp. 1–4, doi: 10.1109/ISSCS.2019.8801753, Jul. 2019- ***indexat WoS*** și ***IEEE Xplore.***

[LO6] **A. Constantin**, R. Tamas, *Impact Reduction of Common Mode Currents for Field Measurements on Directional Symmetrical Antennas, 10th SPIE Conference on Advanced Topics in Optoelectronics*, **in Proceedings SPIE 11718, Advanced Topics in Optoelectronics, Microelectronics and Nanotechnologies, 1171838,** doi: 10.1117/12.2573322, Aug. 2020, Constanta, Romania, SPIE Tracking No. OMN100-148- ***indexat WoS***.

6.4 Future research areas

Future work will focus on:

1. Improving accuracy by:
   a) designing a system with robotic arm that moves the measuring antenna in a large number of points, with a high precision
   b) complete calibrating the PA (loop antenna) taking into account the AUT feeder proximity.
2. Applying the proposed methods in an anechoic chamber below its lower frequency.

Bibliography

[1] C. R. Paul and D. R. Bush, "Radiated Emissions from Common-Mode Currents," in *1987 IEEE International Symposium on Electromagnetic Compatibility*, Aug. 1987, pp. 1–7, doi: 10.1109/ISEMC.1987.7570770.

[2] A. V. Vorobyov, J. H. Zijderfeld, A. G. Yarovoy, and L. P. Ligthart, "Impact common mode currents on miniaturized UWB antenna performance," in *The European Conference on Wireless Technology, 2005.*, Oct. 2005, pp. 285–288, doi: 10.1109/ECWT.2005.1617713.

[3] "IEEE Standard Test Procedures for Antennas," IEEE. doi: 10.1109/IEEESTD.1979.120310.

[4] J. D. Krieger, E. H. Newman, and I. J. Gupta, "The Single Antenna Method for the Measurement of Antenna Gain and Phase," *IEEE Trans. Antennas Propagat.*, vol. 54, no. 11, pp. 3562–3565, Nov. 2006, doi: 10.1109/TAP.2006.884309.

[5] S. Loredo, G. Leon, S. Zapatero, and F. Las-Heras, "Measurement of Low-Gain Antennas in Non-Anechoic Test Sites through Wideband Channel Characterization and Echo Cancellation [Measurements Corner]," *IEEE Antennas Propag. Mag.*, vol. 51, no. 1, pp. 128–135, Feb. 2009, doi: 10.1109/MAP.2009.4939035.

[6] C. Lemoine, E. Amador, P. Besnier, J. Sol, J.-M. Flocrh, and A. Laisne, "Statistical estimation of antenna gain from measurements carried out in a mode-stirred reverberation chamber," in *2011 XXXth URSI General Assembly and Scientific Symposium*, Istanbul, Aug. 2011, pp. 1–4, doi: 10.1109/URSIGASS.2011.6050694.

[7] R. D. Tamas, D. Deacu, G. Vasile, and C. Ioana, "A method for antenna gain measurements in nonanechoic sites," *Microw. Opt. Technol. Lett.*, vol. 56, no. 7, pp. 1553–1557, Jul. 2014, doi: 10.1002/mop.28386.

[8] K. Suto and A. Matsui, "Effects of the common mode on radiation patterns of the tapered slot antenna," in *2017 International Symposium on Antennas and Propagation (ISAP)*, Phuket, Oct. 2017, pp. 1–2, doi: 10.1109/ISANP.2017.8228749.

[9] M. Alexander, T. H. Loh, and A. L. Betancort, "Measurement of electrically small antennas via optical fibre," in *2009 Loughborough Antennas Propagation Conference*, Nov. 2009, pp. 653–656, doi: 10.1109/LAPC.2009.5352516.

[10] C. Balanis, *Antenna Theory Analysis and Design*, 3rd ed. New Jersey: John Wiley & Sons, Inc, 2005.

[11] A. Constantin, L. Anchidin, and R. D. Tamas, "A Distance Averaging Approach for Measuring the Radiation from Common Mode Currents on Antenna Feeders," in *2020 International Workshop on Antenna Technology (iWAT)*, Feb. 2020, pp. 1–4, doi: 10.1109/iWAT48004.2020.1570612231.

[12] L. Anchidin, R. D. Tamas, G. Caruntu, and C.-A. Ilie, "Near-Field Gain Measurements Using the Distance Averaging Method: Linear Scanning Versus Matrix Scanning," in *2018 USNC-URSI Radio Science Meeting (Joint with AP-S Symposium)*, Jul. 2018, pp. 107–108, doi: 10.1109/USNC-URSI.2018.8602746.

[13] Tian Jin, Zhang Linxi, Li Nanjing, and Chen Weijun, "Time-Gating Method for V/UHF Antenna Pattern Measurement inside an Anechoic Chamber," in *2008 International Conference on Microwave and Millimeter Wave Technology*, Apr. 2008, vol. 2, pp. 942–945, doi: 10.1109/ICMMT.2008.4540561.

[14] A. Constantin, L. Anchidin, R. D. Tamas, and G. Caruntu, "A New Method to Reduce the Impact of the Common Mode Currents for Field Measurements on Symmetrical Antennas," in *2019 International Workshop on Antenna Technology (iWAT)*, Mar. 2019, pp. 87–90, doi: 10.1109/IWAT.2019.8730606.

[15] A. Constantin and R. Tamas, “Impact reduction of common mode currents for field measurements on directional symmetrical antennas,” in *Advanced Topics in Optoelectronics, Microelectronics and Nanotechnologies X*, Dec. 2020, vol. 11718, p. 1171838, doi: 10.1117/12.2573322.

[16] A. Constantin and R. D. Tamas, “Evaluation and Impact Reduction of Common Mode Currents on Antenna Feeders in Radiation Measurements,” *Sensors*, vol. 20, no. 14, Art. no. 14, Jan. 2020, doi: 10.3390/s20143893.

[17] A. Constantin and R. D. Tamas, “Loop probe calibration for radiation measurements from common mode currents,” in *2019 International Symposium on Signals, Circuits and Systems (ISSCS)*, Jul. 2019, pp. 1–4, doi: 10.1109/ISSCS.2019.8801753.

[18] L. Anchidin, R. D. Tamas, A. Androne, and G. Caruntu, “Antenna gain evaluation based on weighting near-field measurements,” in *2017 International Workshop on Antenna Technology: Small Antennas, Innovative Structures, and Applications (iWAT)*, Mar. 2017, pp. 78–81, doi: 10.1109/IWAT.2017.7915322.

[19] K. Lin and Y. Lin, “Printed log-periodic dipole antenna with an embedded UWB balun,” in *2012 Asia Pacific Microwave Conference Proceedings*, Dec. 2012, pp. 1361–1363, doi: 10.1109/APMC.2012.6421920.